

## Why are metal foams stable?

Astrid Haibel, Alexander Rack, and John Banhart<sup>a)</sup>

Hahn-Meitner-Institut Berlin, Glienicke Str. 100, 14109 Berlin, Germany and Technical University Berlin, Hardenbergstr. 36, 10623 Berlin, Germany

(Received 3 July 2006; accepted 17 August 2006; published online 10 October 2006)

Although metal foams are becoming accepted engineering materials, the reason for their stability in the liquid state is still under dispute. Liquid metal foams contain solid constituents which according to the existing models stabilize foam films by either modifying the curvature of the liquid/gas (*L/G*) interfaces, or by forming particle bridges across metallic films and transmitting repulsive “disjoining” forces mechanically. Using high-resolution synchrotron tomography and a quantitative three-dimensional image analysis the authors show that there is little evidence for such curvature changes or particle bridges. The authors conclude that the main stabilizing action must be due to interactions between neighboring particles attached to *L/G* interfaces. © 2006 American Institute of Physics. [DOI: 10.1063/1.2357931]

Solid metallic foams are produced by dispersing a large number of gas bubbles into a metallic melt, allowing them to arrange, and freezing the structure by solidification.<sup>1</sup> All production routes for aluminum alloy foams have in common that the liquid alloy has to contain solid particles since pure metallic melts cannot be blown to stable foams. The way how these solid constituents act in a liquid metal foam is still under dispute. Often an analogy to aqueous foams is postulated which are stabilized by surfactants interacting across thin films. This does not lead very far since both attractive van der Waals and repulsive electrostatic interactions acting in aqueous films cannot be found in the much thicker (tens of micrometers instead of tens of nanometers) and electrically conducting metal films. Recently attention has been drawn to aqueous foams and emulsions stabilized by particles without any surfactant being involved<sup>2,3</sup> but, unfortunately, their stability is not yet fully understood either.

Figure 1 explains the stabilization problem. According to Fig. 1(a) flat metallic films are connected to a network of Plateau borders which meet in nodes, the topology being governed by Plateau’s rules.<sup>4</sup> Surface tension  $\sigma$  together with the difference in curvature between films and Plateau borders creates a pressure difference  $\Delta p = 2\sigma(R_{PB}^{-1} - R_F^{-1}) \approx 2\sigma R_{PB}^{-1}$  which—assisted by gravity—tends to remove liquid until the films become unstable unless there is some stabilizing mechanism. The model represented by Fig. 1(b), stating that partially wetting particles are bridged by the melt which then forms menisci of a radius  $R_F \approx R_{PB}$ , thus reducing capillary suction and hampering removal of liquid, seems not realistic looking at real metal foams [Fig. 2(a)]. An alternative model [Fig. 1(c)] postulates that all liquid/gas (*L/G*) interfaces are covered by separate layers of particles which give rise to local menisci between adjacent particles, thus reducing capillary suction. An idea which has recently become popular in metal foam literature<sup>9,10</sup> assumes that opposing particle-covered *L/G* interfaces are mechanically connected by particle bridges across films [Fig. 1(d)], providing repulsive mechanical forces keeping the two *L/G* interfaces apart. A further approach [Fig. 1(e)] postulates that the solid particles increase viscosity so that the melt is largely immobilized.

We make foams from the alloy Al-10 wt % Si-1 wt % Mg containing 10 vol % silicon carbide (SiC, mean particle size of 13  $\mu\text{m}$ ). Precursors were manufactured at the University of Cambridge by admixing 0.5 wt % titanium hydride powder ( $\text{TiH}_2$ , mean particle size of 25  $\mu\text{m}$ ) to the molten alloy, after which the mixture was solidified.<sup>11</sup> For foaming the precursor samples were heated up to about 570 °C, triggering the release of hydrogen gas from the  $\text{TiH}_2$  particles into the melt and generating a foam with a final porosity of  $\approx 70\%$ .

The light microscopic section of a solidified foam film [see Fig. 2(a)] shows an agglomeration of dark SiC particles at the metal/gas boundaries. Only few particles are found in the interior of the films, most of them attached to the eutectic. No surface modulations as claimed by the models depicted in Figs. 1(b) and 1(c) can be detected. The top view of the same film displayed in Fig. 2(b) shows that a large fraction of the surface is covered by particles. Figure 2(a) does not yield any evidence for particle bridges between the two interfaces of the film. However, as particle bridges are not necessarily parallel to the plane of view, a three-dimensional (3D) investigation is necessary.

Tomography was carried out at the synchrotron BESSY in Berlin. X rays monochromatized to 25 or 30 keV passed through the samples and were converted to visible light by  $\text{Gd}_2\text{O}_2\text{S}$  or yttrium aluminum garnet doped  $\text{Ce}^{3+}$  scintillators. The optically magnified images were captured by a 2048  $\times$  2048 pixel charge-coupled device camera. For each tomo-

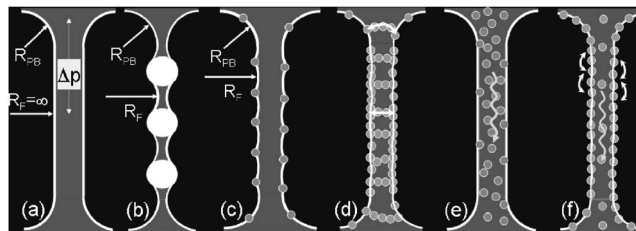


FIG. 1. (a) Liquid film in a foam.  $R$  denotes radii of curved films and  $\Delta p$  the pressure difference within a film. [(b)–(f)] Different models for foam stability: (b) adsorbed particles bridged by film (Ref. 5), (c) interfaces modulated by adsorbed particles (Ref. 6), (d) particle layers on interfaces mechanically connected by bridges (arrows: forces) (Ref. 7), (e) drainage reduction by particles (arrow: flow) (Refs. 1 and 8), and (f) model proposed in this letter.

<sup>a)</sup>Electronic mail: banhart@hmi.de

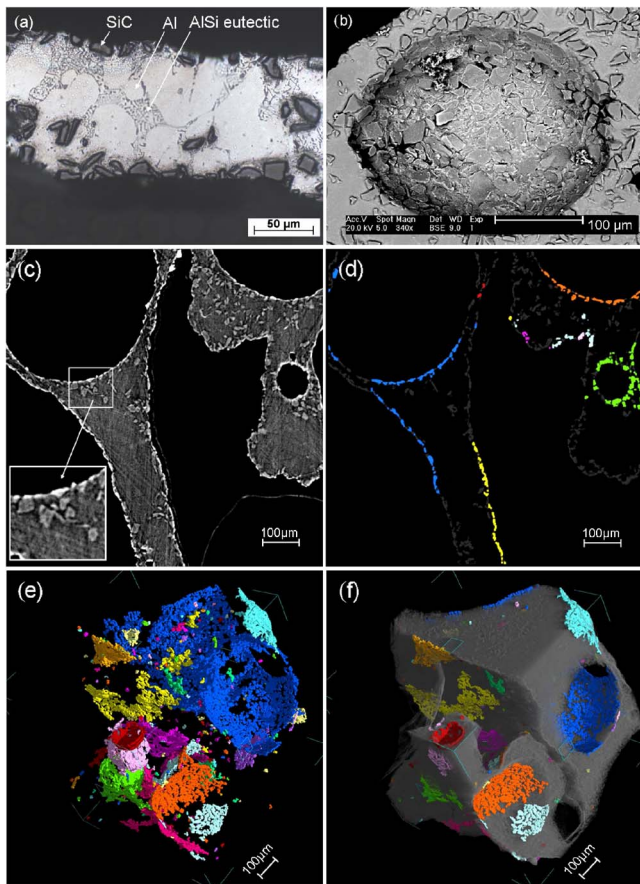


FIG. 2. (Color online) Images of solid aluminum foam: (a) light microscopic view of polished section, (b) scanning electron microscopic top view of a pore interior, (c) tomographic image of plane through foam, (d) same plane image processed (large groups of connected particles are color coded, small groups are shown in gray), (e) 3D visualization of connected particle clusters, and (f) same as (e) but showing the aluminum matrix. [(c)–(f)] Pixel size of  $1.5 \mu\text{m}$ , energy of  $25 \text{ keV}$ , and box length 600 pixels.

gram 900 radiograms with pixel sizes of  $1.5$  or  $3.6 \mu\text{m}$  were obtained which took about 25 min. Tomographic reconstruction yielded a 3D data set representing the local mass distribution in the sample. As the absorption coefficients of the alloy and the SiC particles are very similar ( $5$  and  $5.7 \text{ cm}^{-1}$ , respectively, at  $E=25 \text{ keV}$ ) it is the diffraction effects at the metal/particle boundaries that enable us to distinguish between the two components.<sup>12</sup>

Figure 2(c) shows a two-dimensional (2D) slice from a 3D tomogram of a solid foam. The SiC particles decorate the surfaces of the cell walls in accordance with the light optical micrograph. For a connectivity analysis of the SiC particles, i.e., to check whether the particles form continuous layers, bridges, or even networks in the metallic matrix, bubbles and particles were separated and Boolean images created. Objects consisting of connected particles were identified by an algorithm—implemented in the commercial package MAVI—which isolates all topologically connected regions of an image and labels them with a number or, for the purpose of visualization, by a color.<sup>13</sup> We found that the SiC particles in a region of  $600^3$  pixels belonged to about 21 000 distinct groups. Besides many very small ones some contain up to 2600 particles. The 15 largest groups covering the metal/gas interfaces were color coded and are shown in Figs. 2(d)–2(f). It is obvious that layers covering opposite interfaces are not necessarily connected. The long film in the lower middle of

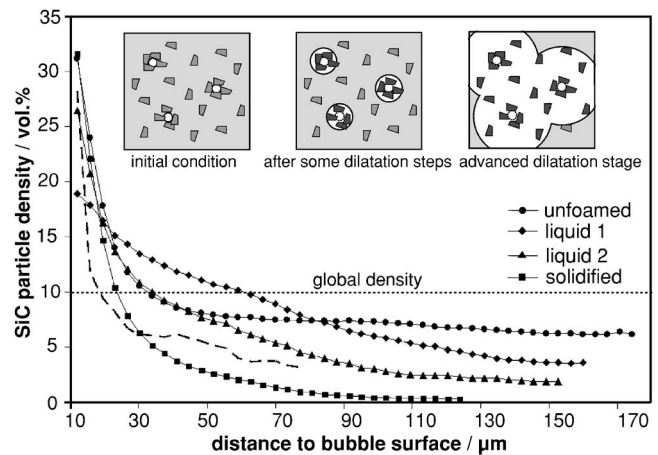


FIG. 3. Correlation between bubbles and stabilizing SiC particles. Mean SiC density given as a function of mean distance to bubble surface for the unfoamed solid precursor, the liquid foam in two stages (1/2), and the solidified foam. Pixel size of  $3.6 \mu\text{m}$  and x ray energy of  $30 \text{ keV}$ . The broken line corresponds to the foam in Fig. 2(c). Inset: Sketch of bubble dilatation procedure (Al: light gray, bubbles: white, SiC: dark gray).

Fig. 2(d), e.g., does not contain a single bridge between the two layers which therefore appear in different colors. Some connections are observed (e.g., for the blue component), but this case is an exception. Figures 2(e) and 2(f) display 3D visualizations of the same sample and confirm the interpretation of the 2D slice.

A fundamental problem in our investigation is that an interpretation of phenomena in the liquid state is given after solidification. Solidifying metal can push or engulf particles depending on their size, solidification rate, and other factors. Hypothetically, particle bridges could exist in the liquid state but be destroyed during solidification so that our previous analysis would not have detected them. In order to investigate particle rearrangements during foaming and solidification we studied liquid metal foams by *in situ* tomography. The unfoamed precursor was heated by two lamps, melted and foamed, after which tomographic images were obtained. A lower magnification was applied to allow for a reasonable sample size. We were able to obtain two sufficiently undistorted images of a liquid foam in addition to images prior and after foaming. The time span between subsequent measurements was 25 min.

From the resulting four 3D data sets spatial correlations between bubbles and SiC particles were determined by dilating the bubble volumes (shown in white in the inset of Fig. 3) in equidistant steps starting from the initial surface. After each dilatation step those pixels contained in the incremental bubble volume and corresponding to SiC were marked and counted, from which a SiC density in the incremental volume was calculated (Fig. 3; data corresponding to Fig. 2 are also shown to demonstrate that different image resolutions do not have much influence on the results.) A statistical distribution of SiC particles in the Al matrix would lead to a constant value: the global density of 10%. This is not the case in any of the four curves. The SiC density is always high close to bubbles and drops monotonously with distance indicating a spatial correlation between bubbles and particles. In the precursor sample the local SiC concentration is 31.5% close to the  $L/G$  interfaces, for more than  $40 \mu\text{m}$  distance the concentration is nearly constant ( $\approx 7\%$ ). We suspect that gas evolving from the blowing agent during

manufacture of the precursor preferentially attaches to SiC particles, leading to this correlation, in analogy to the description in Ref. 14. Foaming clearly leads to a redistribution of particles. In the vicinity of the bubbles the SiC density rises (after an initial decrease, caused by the large bubble inflation in early foaming stages) while at larger distances it drops, indicating an ongoing rearrangement of particles from the film interior to the  $L/G$  interfaces. The interface concentration after solidification goes up to 32%, compatible with values given in the literature.<sup>5,15</sup>

Interestingly, the solidified state shows a more pronounced correlation than the second stage of the liquid. A part of this correlation increase can be ascribed to rearrangements before solidification, but part of it might be caused by the pushing of particles to the  $L/G$  interfaces by the solidification front. A connectivity analysis in the liquid state—not feasible due to the insufficient resolution of our measurements—would possibly lead to the identification of more connected particles than in the solid. However, in view of the still low particle densities in the middle of the liquid films, i.e.,  $\approx 5\%$  at  $75\ \mu\text{m}$  distance from the interfaces, we consider it unlikely that bridges being able to transmit mechanical forces can be formed.

Our analysis shows that particles do not interact across liquid metal films, e.g., there is no analog to the “disjoining pressure” known to stabilize aqueous foams as claimed by several researchers.<sup>7,9,10</sup> Instead, liquid metal foams must be stabilized by interactions between particles attached to one side of a film. In aqueous foams such interactions can be both repulsive and attractive,<sup>16</sup> the origin of these interactions, however, being still under debate (see, e.g., Refs. 17 and 18). Analogous interactions between SiC particles could create the surface elasticity needed to prevent rupture in metallic films. In addition, particles within individual films may contribute to stabilization by increasing the apparent viscosity. Figure 1(f) summarizes this conclusion schematically.

Future optimization of metal foam stability should be directed towards improving the interactions between particles on metal films instead of attempting to increase the particle content in the metal bulk. The use of nanoparticles could allow for making stable metal foams containing only a few vol % of nonmetallic additions.

The authors acknowledge cofunding by the European Space Agency, MAP AO99-075. Samples were kindly provided by V. Gergely, University of Cambridge, U.K. H. Riesemeier, J. Goebbels, and G. Weidemann are thanked for their technical support.

<sup>1</sup>J. Banhart, *J. Met.* **52**, 22 (2000).

<sup>2</sup>B. P. Binks, *Curr. Opin. Colloid Interface Sci.* **7**, 21 (2002).

<sup>3</sup>R. J. Pugh, *J. Complex.* **114-115**, 239 (2005).

<sup>4</sup>D. Weaire and S. Hutzler, *The Physics of Foams* (Oxford University Press, London, 1999).

<sup>5</sup>S. W. Ip, Y. Wang, and J. M. Toguri, *Can. Metall. Q.* **38**, 81 (1999).

<sup>6</sup>H. Kumagai, Y. Torikata, H. Yoshimura, M. Kato, and T. Yano, *Agric. Biol. Chem.* **55**, 1823 (1991).

<sup>7</sup>G. Kaptay, *Colloids Surf., A* **230**, 67 (2004).

<sup>8</sup>V. Gergely and T. W. Clyne, *Acta Mater.* **52**, 3047 (2004).

<sup>9</sup>C. Körner, M. Arnold, and R. F. Singer, *Mater. Sci. Eng., A* **396**, 28 (2005).

<sup>10</sup>T. Wübber and S. Odenbach, *Colloids Surf., A* **266**, 207 (2005).

<sup>11</sup>V. Gergely and T. W. Clyne, *Adv. Eng. Mater.* **2**, 168 (2000).

<sup>12</sup>P. Cloetens, M. Pateyron-Salomé, J. Y. Buffière, G. Peix, J. Baruchel, F. Peyrin, and M. Schlenker, *J. Appl. Phys.* **81**, 5878 (1997).

<sup>13</sup>G. Lohmann, *Volumetric Image Analysis* (Wiley, Chichester/Teubner, Stuttgart, 1998).

<sup>14</sup>L. Helfen, T. Baumbach, P. Cloetens, P. Pernot, H. Stanzick, K. Schladitz, and J. Banhart, *Appl. Phys. Lett.* **86**, 231907 (2005).

<sup>15</sup>N. Babszán, D. Leitmeier, and J. Banhart, *Colloids Surf., A* **261**, 123 (2005).

<sup>16</sup>P. A. Kralchevski and K. Nagayama, *Adv. Colloid Interface Sci.* **85**, 145 (2000).

<sup>17</sup>M. G. Nikolaidis, A. R. Bausch, M. F. Hsu, A. D. Dinsmore, M. P. Brenner, C. Gay, and D. A. Weitz, *Nature (London)* **420**, 299 (2002).

<sup>18</sup>M. Megens and J. Aizenberg, *Nature (London)* **424**, 1014 (2003).